International Journal of Hydrogen Energy 66 (2024) 81–89

Contents lists available at ScienceDirect

International Journal of Hydrogen Energy

journal homepage: www.elsevier.com/locate/he

Ignition delay of lean hydrogen-air mixtures

Pavel Krivosheyev [a,*], Yuliya Kisel [a], Alexander Skilandz [a], Kirill Sevrouk [a], Oleg Penyazkov [a], Anatoly Tereza [b]

[a] A.V. Luikov Heat and Mass Transfer Institute, National Academy of Sciences of Belarus, Minsk, Belarus
[b] Semenov Federal Research Center for Chemical Physics, Russian Academy of Sciences, Moscow, Russia

ARTICLE INFO

Handling editor: J Lobato

Keywords:
Lean hydrogen-air mixture
Self-ignition
Ignition delay
Shock tube
Detailed kinetic mechanism
Modelling

ABSTRACT

The ignition of lean hydrogen-air mixtures behind reflected shock waves at the temperature range of 902–1630 K and the pressure of 1 atm is studied experimentally and numerically. For the first time, reliable experimental data is obtained for temperatures below 1000 K, directly in the zone of change in the dominance of chain branching and chain termination reactions, which influence the formation of the ignition delay value. Expressions are formulated for ignition delay in two temperature intervals below and above 970–980 K, and the corresponding activation energy values are determined. Good agreement between the experimentally observed and calculated ignition delay values is demonstrated. The local sensitivity analysis allowed us to reduce the kinetic mechanism.

1. Introduction

The high proportion of electrical energy generated by nuclear power plants (NPP) requires increased safety requirements for nuclear reactors in the context of natural and man-made disasters. When developing new methods for increasing fire and explosion safety at water-cooled nuclear power plants and related design solutions, one of the most relevant challenges is predicting the autoignition and combustion of lean and ultra-lean hydrogen-air mixtures [1–4]. The events that unfolded at Chernobyl and Fukushima Daiichi demonstrated that one of the causes of the accidents was the formation of molecular hydrogen [5,6]. The exceedance of concentration limits for autoignition and flame propagation in the hydrogen-air mixture led to an uncontrolled explosive effect, which resulted in the destruction of the structures of NPP units.

The most likely mode of combustion of gas mixtures within the regions of ignition instability is deflagration. In the deflagration mode, flame propagates through the mixture consisting of fuel and oxidizer due to heat transfer and diffusion transfer of active radicals from the reaction zone. It is well known that such a combustion mode is subject to numerous instability factors of various nature. When it develops in an enclosed volume, the deflagration wave can accelerate under the influence of gas-dynamic processes determined by the combustion itself. In turn, flame acceleration leads to the formation of compression waves or even detonation waves resulting from the deflagration-to-detonation transition. As a rule, scenarios of intense flame acceleration and transition to detonation are regarded as the most destructive ones [7]. All the consecutive stages of flame development, mechanisms and scenarios for the occurrence of detonation on a laboratory scale (in channels) have been described in recent experimental [8–12] and theoretical-and-calculation [13–17] studies. In [18], it was demonstrated that under the conditions of explosive ignition of a hydrogen-air mixture, the optimal upper limit of pressure in an enclosed volume of the structure of a NPP unit amounts to 6 atm. As a result, the study of ignition, flame propagation and the transition of combustion to detonation shall be objectively studied at the pressure range of 1–6 atm. With regard to the tasks of ensuring fire and explosion safety at nuclear power plants, carrying out full-scale tests for the study of combustion of hydrogen-air mixtures is troublesome due to the huge geometric dimensions of the object itself, therefore, a computational experiment method comes to the fore. At the same time, in addition to the modelling of gas-dynamic processes inside the plant containment, it is important to correctly select and use an adequate detailed kinetic mechanism (DKM) or model of hydrogen oxidation in order to describe its combustion and detonation (including detonation cell structure) as shown in recent publications [19–21].

One of the key parameters by which detailed kinetic mechanisms are validated is the ignition delay time (IDT) (τ), which shall be determined at $V = \text{const}$, given the enclosed volume of NPP units. Numerous studies

* Corresponding author.
E-mail address: krivosheyev.pavlik@gmail.com (P. Krivosheyev).

https://doi.org/10.1016/j.ijhydene.2024.03.363
Received 6 December 2023; Received in revised form 11 March 2024; Accepted 29 March 2024
Available online 11 April 2024

have been devoted to the experimental determination and numerical description of IDT in the ignition of hydrogen-air-oxygen mixtures [22–37]. In the review [28], it was demonstrated that the scatter of the experimentally obtained ignition delay (τ) values is orders of magnitude in the region of T = 1000 K. The reasons for such discrepancies in experimental data are related to gas-dynamic effects that affect the accuracy of measurements [27,28,38,39], the presence of impurities [32,40–42], and with increasing pressure, the influence of quantum corrections on elementary reaction rate constants [43]. At the same time, the development of kinetic models of ignition and combustion of hydrogen-air mixtures has shown that, in general, they agree well with each other in the pressure range of 1–6 atm for lean mixtures, which are most relevant in the study of fire and explosion safety at nuclear power plants [2]. The greatest discrepancies between various numerical models presented in the literature for the ignition of hydrogen-air mixtures are observed in the temperature region of 930 K at the pressure of 1 atm and 1100 K at 6 atm [2]. Namely, in the region of these temperatures there is a pronounced competition between chain branching and chain termination reactions, which is designated as "cross-over" in the literature [44]. It is was found that the cross-over temperature that appears in the cutoff factor is smaller under fuel-rich conditions [45]. As pressure increases well above 6 atm, quantum effects may need to be taken into account to describe experimental data [43].

Since the block of reactions with hydrogen is included as a submechanism in the general mechanism of oxidation of any hydrocarbon, not only kinetic mechanisms of oxidation of pure hydrogen mixtures (mainly at high pressures) [34,36,46–51], but also the influence of various additives [32,52–56]] or ignition of syngas fuels [29,57–59] are intensively studied. However, not many publications on the ignition of lean hydrogen mixtures, especially at low pressures, can be found in the literature, one of them is [34] for H_2/O_2 mixtures diluted with argon over the temperatures from 850 K to 1500 K, the pressures from 1.2 to 16.0 atm, and the equivalence ratios of 0.5, 1.0 and 2.0.

It should be noted that the development of methods of quantum-mechanical calculations of the rate constants of elementary reactions gives reason to assert the role of the influence of a number of leading channels that determine the autoignition of hydrogen-air mixtures. Having carried out numerical and theoretical analysis of transition states of three H_2+O_2 initiation reactions, the authors [60] made a statement about the dominance of one of them. The numerical modelling of own experimental results allowed to confirm this statement within the limits of experimental errors allowed by the authors. At the same time, in [32], based on the description of their own experimental and literature data, the statement of the paper [60] was questioned. Based on recent literature data on the rate constants of elementary reactions and seeking to improve the description of self-ignition of hydrogen-air mixtures and laminar flame propagation through them A. Konnov [48] not only replaced the rate constants of the three reactions, but also greatly expanded the mechanism by introducing new species that can occur under certain physicochemical conditions.

To more accurately construct kinetic models of ignition of lean hydrogen-air mixtures, especially at relatively low temperatures (T < 1000 K), it is necessary to obtain reliable experimental data. The purpose of this study was to obtain a large array of experimental results on the self-ignition of lean (less than 10% by volume) hydrogen-air mixtures at the widest possible temperature range and initial atmospheric pressure behind reflected shock waves.

2. Experiment and simulation details

2.1. Experimental setup

To obtain the most reliable data, the studies were carried out simultaneously using two experimental setups representing shock tubes with an internal diameter of 50 and 76 mm, respectively.

Fig. 1 shows characteristic measuring sections and the distances between them. All measuring sections, including those located at the end of the tubes (end wall flanges), were equipped with high-frequency pressure transducers manufactured by PCB Piezotronics (model 113b24 and 113b26) with response time less than 1.5 μs and with a 1.5-mm spatial resolution, and ionization sensors. The reaction luminescence is recorded by photoelectronic multipliers or photomultiplier tube (PMT). The time resolution and linearity of the characteristics of ionization sensors were verified by shorting to a resistance of a certain value, and for PMT – with the use of pulsed LED light. Time resolution for PMT amounted to 0.6 μs and for the ionization sensors – to 0.15 μs. Signals were recorded at a frequency of 10 MHz.

In addition to the diameter, optical observation schemes for the two installations had some other differences. A cylindrical shock tube with an internal diameter of 50 mm had a length of 8.5 m. Its measuring section (Fig. 1a) with a square outer cross-section and the end wall flange were made of SO-95 transparent organic glass with a softening temperature of 95 °C. Its transmittance of UV radiation at a wavelength of 309 nm amounted to 20%. From the end of the tube, chemiluminescence of the transition ($A^2\Sigma - X^2\Pi$) was recorded at a wavelength λ = 308.9 nm, which is characteristic of the excited intermediate radical OH*. The radiation of the reacting mixture through a Ø 2 mm diaphragm and a dual light filter (308 nm with a half-maximum width of the transmission contour of 1.4 nm) reach the PMT located at a distance of 200 mm from the end. Thus, the radiation was recorded from a solid angle of 0.244 rad (a cone with an angle of 14°).

The cylindrical shock tube with a diameter of 76 mm had a length of 6.5 m. The tube flange was made of SO-95 organic glass with a softening temperature of 95 °C. Its transmittance of UV radiation at a wavelength of 309 nm amounted to 20%. The light from the reacting mixture (Fig. 1b) was collected from the volume of the measuring section using a lens with a focal length of 500 mm made of KU-1 glass. Focusing was accomplished by constructing an image of a sharp line contour on a luminous background located at a distance of 6.8 m (13.6 * F) from the lens. The light was focused on the PMT diaphragm. The distance from the centre of the lens to the PMT diaphragm was 490 mm. The PMT diaphragm had a diameter of 2 mm. In the infinity focusing approximation, the light was collected from a solid angle of $1.26*10^{-5}$ rad (a cone with an angle of 0.23°) with a one-sided divergence of 2 mm/m. Next, a light filter was installed on the PMT. A narrow-band light filter 309BP1.5 No. 210898 (Omega, USA) with a centre of 309 nm and a half-maximum width of the transmission contour of 1.5 nm was used.

The ignition of ultra-poor hydrogen-air mixtures (φ = 0.15 and φ = 0.25, where φ is the equivalence ratio) behind a reflected shock wave was studied. The mixtures were prepared in advance in separate cylinders using a manometric method and kept for at least 24 h before use. Helium was used as a pushing gas in the high-pressure chambers of the shock tubes. Immediately before the experiments, the low-pressure chambers of the shock tubes were vacuumed to a residual pressure of no more than 100 Pa, then flushed with the mixture under study and vacuumed again.

The studied mixtures and test conditions are given in Table 1.

The main measurement uncertainties were associated with several factors. The first one is impurities in gases and uncontrolled external air leakage into shock tube during test preparation time. Commercial grade hydrogen, oxygen and nitrogen of 99.99% chemical purity were used for mixtures preparations. The rate of leakage into the tube during test preparation time was no more than several tens of Pa. Combined, this resulted in a mixture composition error no more than 0.1–0.2 %. The second one is an uncertainty in incident shock-wave velocity measurements at different locations along the tube, related with pressure sensors spatial resolution (1.5 mm), distances between sensors at the measuring bases (70–100 mm) and sampling frequency of the recording equipment (1–5 MHz). Usually, this can result in a 0.5–1.0 % error in incident shock-wave velocity measurements, which produces no more than 1–2 % errors in calculated parameters of temperature, pressure and density

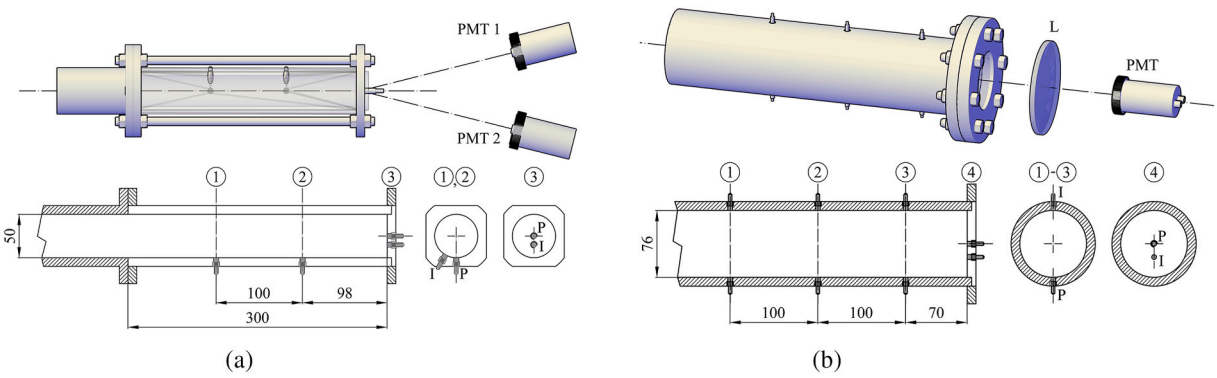

Fig. 1. Measuring sections of a shock tube with a diameter of 50 mm (a) and 76 mm (b). Numbers 1–4 represent measuring sections with ionization (I) sensors and pressure (P) transducers, stands for photomultiplier tube with a diaphragm and dual narrow-band filters (L).

Table 1
Experimental conditions.

φ, equivalence ratio	Mixture	Internal diameter of the tube, d, mm	Pressure behind the reflected shock wave P, MPa	Temperature behind the reflected shock wave T, K
0.15	5.93% H_2+19.76% O_2+74.31% N_2	50	0.102 ± 0.013	940–1553
		76	0.099 ± 0.006	902–1630
0.25	9.5% H_2+19% O_2+71.5% N_2	50	0.103 ± 0.008	929–1544
		76	0.101 ± 0.009	904–1563

of the mixture behind reflected shock waves.

2.2. Ignition delay time measurements

Self-ignition of the gas mixture under study and measurement of the induction time occurred behind the shock wave reflected from the end of the measuring section. All experiments were performed at a constant density behind the reflected shock wave in order to obtain the correct temperature dependence of the induction time on the activation energy of the mixture and the concentrations of fuel and oxidizer. This means that the concentrations of hydrogen, oxygen and nitrogen behind the reflected shock wave were maintained almost constant during the induction period in each section of the shock tube for the entire temperature range under study.

Fig. 2 Demonstrate typical end-wall pressure and luminescence histories from both experimental facilities. The time of arrival of the incident shock wave at the end reflecting flange determined from the oscillogram of the pressure sensor mounted in the flange was taken as the "zero count" of time when determining the ignition delay.

The velocity of the incident shock wave was determined by the time of its arrival at the corresponding measuring section, by analyzing the pressure profiles. Gas parameters behind incident and reflected shock waves were determined on the basis of incident shock wave velocity measurements from the 1D shock relations assuming vibrational equilibrium, frozen chemistry and known temperature dependence of heat capacity. The detailed description and calculation procedure can be found in Supplementary materials # 1.

The luminescence induction times were determined as follows. Since the radiation was collected from the entire volume of the tube, the final glow signal was integral over time; the glow from each subsequent volume of the reacting mixture (tube cross-section) was superimposed and summed with the previous one. Due to the low luminosity of the recorded reaction, which is also associated with the low value of the equivalence ratio of the mixtures under study, the recorded signals of the photomultiplier were very noisy, which introduced a significant error in the results of measuring the ignition delay directly, for example, from the beginning of growth or from the peak of the original signal. To more accurately measure the ignition delay, the following procedure was used. Initially, the original signals were smoothed using the fast Fourier transform. In doing so, filters were used that effectively let through the frequency spectrum of the signal below a certain frequency and suppressed signal frequencies above the same frequency. For each signal, the indicated cut-off frequencies were selected individually, depending on the type of specific signal and the respective signal-to-noise ratio. After smoothing the original signal, the first derivative was calculated using the differentiation function. To determine the self-

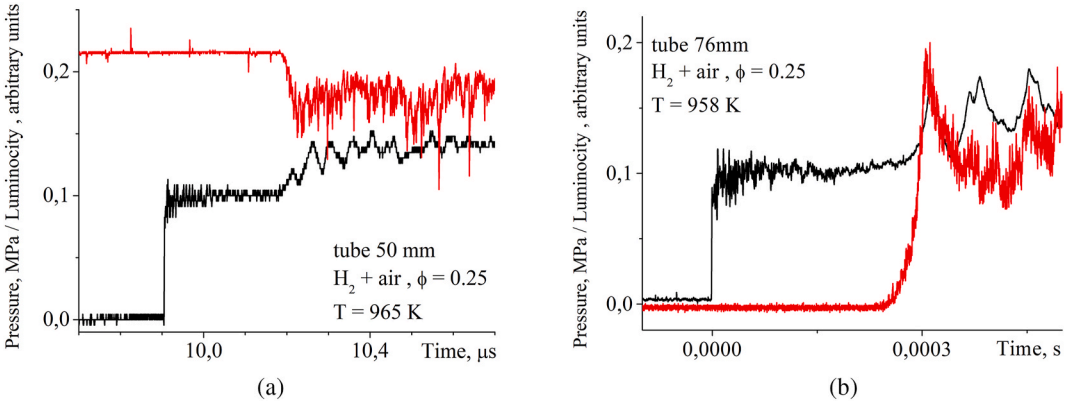

Fig. 2. Typical end -wall pressure (black lines) and luminescence (red lines) of electronically exited OH* radical recorded in experiments.

ignition time, the first minimum/maximum value was marked on the graph of the differentiated signal. Fig. 3 shows typical oscillograms of the glow signals recorded in the experiment and the results of their processing in the manner described above. In the case of an integrated signal recorded from the end of the shock tube, the maximum glow in the cross section corresponds to the point of maximum growth of the integrated signal.

2.3. Simulation details

All calculations were carried out using the CHEMKIN-PRO software product included in the ANSYS package (Academic version) [61]. The choice of the DKMs used was determined by the following factors. Since the experiments recorded the emission signal of the electronically excited radical OH*, only DKMs containing blocks of reactions involving this particle were considered. Moreover, since in general at this temperature and pressure range, lean hydrogen-air mixtures are described by the majority of DKMs with fairly similar results, three DKMs developed by different groups of researchers were selected [29,32,48]. All of them have been tested, and they demonstrated good agreement with experimental data. For all calculations, thermal files in the NASA standard [62] were used, which were supplemented to each of the DKMs used. The ignition delay (τ) values were determined under the condition of V = const at the time point corresponding to the maximum luminescence (peak) of the OH* radical.

3. Results

Fig. 4 shows the resulting dependences of ignition delay on the inverse temperature for lean (φ = 0.15 and φ = 0.25) hydrogen-air mixtures at the temperature range of 902–1630 K and the pressure behind the reflected wave of 1 atm. Detailed data can be found in Supplementary materials # 2. The results obtained for the two experimental setups are presented. It is clearly seen that the measurement results at different installations coincide with each other, which indicates the high quality and reliability of the experimental data obtained, correctly chosen methodology for conducting the tests and processing experimental data. It should be noted that in this study, in fact, it was possible to obtain the ignition delay (τ) values below 1000 K for lean hydrogen-air mixtures for the first time. In the temperature range of 902–1400 K, the agreement on ignition delays is almost perfect. Noteworthy is only a slight difference in the data in the region of high (more than 1400 K) temperatures and, as a consequence, the shortest values of ignition delay. This fact requires separate consideration; a possible reason lies in the influence of gas-dynamic effects, which are more pronounced and manifest themselves in one of the experimental setups.

The presented data for the studied mixtures can be conditionally divided into two groups, each of which is well approximated by a linear dependence. The border line between such data groups is the temperature region of approximately 970–980 K, which corresponds to an area close to the cross-over zone in a laminar flame propagating in a hydrogen-air mixture under normal initial conditions [44]. The following dependencies were obtained:

for a mixture with φ = 0.15 (see Fig. 4a):

at T > 980 K

$$Lg\,(\tau) = -1.01 + 3.19\left(\frac{1000}{T}\right), \text{in which case } E = 61.1$$

at T < 980 K

$$Lg\,(\tau) = -10.74 + 12.71\left(\frac{1000}{T}\right), E = 243.4$$

for a mixture with φ = 0.25 (see Fig. 4b):

at T > 970K

$$Lg\,(\tau) = -1.06 + 3.19\left(\frac{1000}{T}\right), E = 61.1$$

at T < 970K

$$Lg\,(\tau) = -12.96 + 14.86\left(\frac{1000}{T}\right), E = 284.5$$

where:

τ – ignition delay time (μs)
T – temperature of the gas behind the reflected shock wave (K),
E – activation energy ($\frac{KJ}{mole}$).

Fig. 5 shows a comparison of experimental and simulation results for the selected and above-mentioned DKMs. It can be seen that all the kinetic mechanisms used describe the experimental results qualitatively very well. As for the quantitative agreement, the calculation results are close to each other and demonstrate good (within 0.3–0.4 order of magnitude) agreement with the experimental data. It should be noted that in the region of the lowest (below 950 K) and highest (above 1500 K) temperatures, the mechanism described in [48] performs at its best. In the entire remaining temperature range, the results of calculations based on the mechanism described in [32] most closely agree with the experimental data.

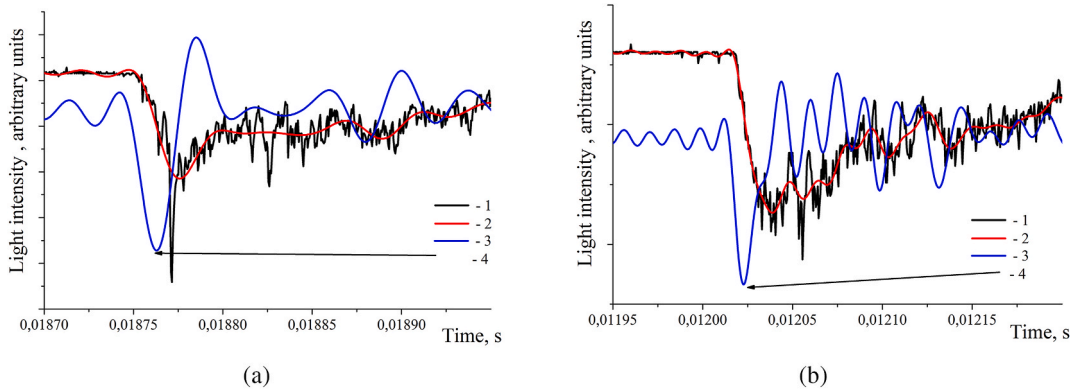

Fig. 3. Typical signals (oscillograms) of a photomultiplier tube recorded in the experiment and the results of their processing to determine the ignition delay time. 1 – original signal, 2 – signal after smoothing with the use of fast Fourier transform, 3 – smoothed signal after differentiation, 4 – position of the peak from which the ignition delay time was determined. Experiment 224 (a) and 264 (b), see Supplementary materials # 2.

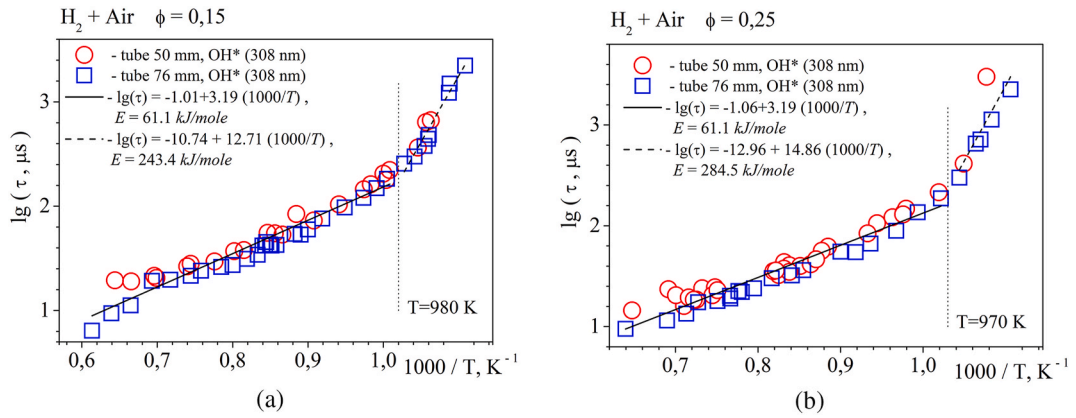

Fig. 4. Ignition delay time versus inverse temperature for lean hydrogen-air mixtures at the temperature range of 902–1630 K and the pressure behind the reflected wave of 1 atm, φ = 0.15 (a) and φ = 0.25 (b).

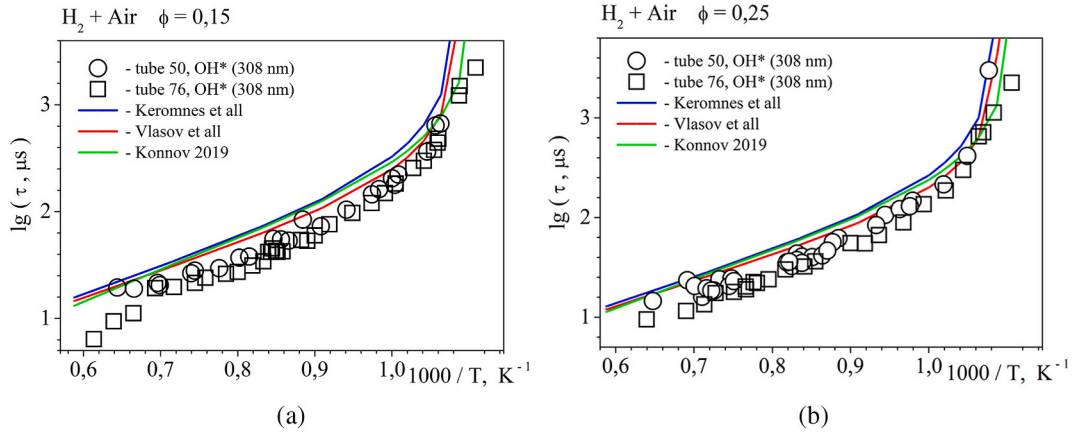

Fig. 5. Ignition delay time versus inverse temperature for lean hydrogen-air mixtures at the temperature range of 902–1630 K and the pressure behind the reflected wave of 1 atm, φ = 0.15 (a) and φ = 0.25 (b). Comparison of experimental results and results of simulation using detailed kinetic mechanisms from refs [29,32,48].

4. Discussion

Fig. 6 shows a comparison of typical profiles of the electronically excited intermediate radical OH*, which were recorded in the experiment, with the results of numerical simulation. For comparison, experiments with both a high temperature (1563 K) at a correspondingly short (less than 10 μs) ignition delay, and as well as experiments with a fairly low (979 K) temperature and an average (187 μs) delay were selected.

As can be seen from Fig. 6, the shape of the simulated OH* profiles in the calculations based on the DKMs described in refs [29,32,48] is the same and closely resembles the profiles recorded in the experiment. At the same time, all calculated OH* curves reach their maximum later than the experimentally observed emission signal of electronically excited hydroxyl. At high temperatures, the times at which the OH* glow reaches its maximum for all three DKMs are quite close to each other (see Fig. 6b). The difference in the time to reach the OH* maximum according to different DKMs is more noticeable at temperatures below 1000 K (see Fig. 6a). Such a discrepancy in calculations based on different DKMs at low temperatures is due to the fact that the ignition delay (τ) value is highly temperature dependent (see Fig. 4 and

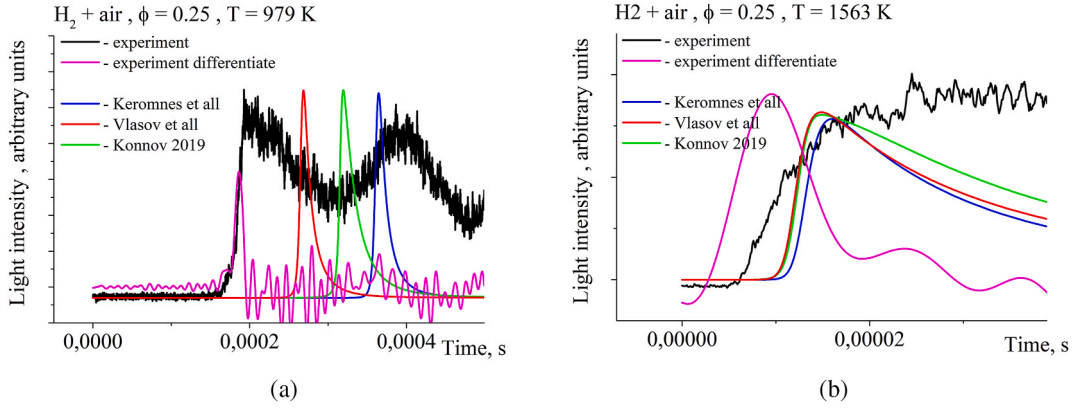

Fig. 6. Comparison of experimentally recorded profiles of the electronically excited intermediate radical OH* with the results of numerical calculations.

the corresponding formulas above). Such a break in the temperature dependence in the region of $T \sim 970$ K corresponds to a change in dominance between the two main channels that determine the branched chain process of self-ignition of the H_2/O_2 mixture [44,45,63], namely, the chain branching reaction

$$H + O_2 = OH + O \quad (R1)$$

and the chain termination reaction

$$H + O_2 + M = HO_2 + M \quad (R2)$$

The sensitivity analysis described in [61] demonstrated that it is these reactions (R1) and (R2) that make the greatest contribution to the formation of the ignition delay (τ) value for ultra-lean mixtures. The value of k_1 decreases with decreasing temperature, while the value of k_2 increases. In the region of $T \sim 970$ K, an equilibrium of sensitivity to the formation of the ignition delay (τ) value is observed between the reactions of (R1) and (R2). It is the difference in the parameters of the rate constants of reactions (R1) and (R2) in different DKMs that predominantly determines the difference in the calculated ignition delay (τ) values. It should be taken into account that at the pressure of 1–6 atm, reaction (R2) occurs in the pressure transition region and the values of k_2 are calculated in the CHEMKIN-PRO module according to J. Troe approximation formulas [64] with the use of limiting values of reaction rate constants (R2) for low (k_0) and high (k_∞) pressure. In different DKMs, not only the Arrhenius parameters of the values of k_0 and k_∞, but also the Troe parameters and Chaperon efficiencies differ. Given that with decreasing temperature the influence of reaction (R2) increases compared to (R1) [44], all these uncertainties in the mentioned parameters introduce a noticeable discrepancy in the calculations of the k_2 value for different DKMs.

To better understand the experimentally observed two groups of temperature dependences of τ with different activation energies up to 970 K and above, we analyzed the local sensitivity of the main pathways of OH radical formation and loss. The hydroxyl radical was chosen because it is one of the main intermediates determining the development of the chain branching process that forms the ignition delay. Sensitivity analysis was performed using DKMs from refs [29,32]. In addition to the difference in the rate constants of some reactions, these mechanisms are distinguished by the presence of a second initiation channel with the formation of two OHs in [32]. The results of the sensitivity analysis are presented in Figs. 7–9. The vertical lines in Figs. 7–9 represent the time moments corresponding to the maximum of OH* emission - $\tau(OH^*_{max})$. Comparing the results of sensitivity analysis by the DKMs from refs [29, 32] one can note the difference only for high temperatures (Fig. 7). At low temperatures (Figs. 7 and 8), the influence of the main reactions on ignition delay is the same for both mechanisms.

Fig. 7a shows the local sensitivity of the main OH formation reactions for high temperature, much higher than 970 K. It can be seen that the main contribution is made by reaction (R1). In addition to it, the following reactions make a noticeable contribution to the rate of growth of OH concentration

$$H_2 + O = H + OH \quad (R3)$$

$$H_2 + OH = H_2O + H \quad (R4)$$

The effects of reactions (R1), (R3), and (R4) on the reduction of τ are simbate and reach their respective maxima at the same time point. At the same time, the reaction

$$OH + OH = H_2O + O \quad (R5)$$

which increases the ignition delay, reaches its maximum influence somewhat later, namely when the influence of reactions (R1), (R3), and (R4) decreases significantly. Note the very weak influence of the reaction (R2), which first increases the value of τ and then actually with the same weight leads to its decrease. In this case, the maximum influence of reaction (R2) on the increase of τ coincides in time with the moment of the maximum influence of reactions (R1), (R3), and (R4). The time moment of maximum OH* luminescence for the conditions of Fig. 6b corresponds to the value $\tau(OH^*_{max}) = 14.9$ μs (Fig. 7a), which according to Fig. 7a corresponds to the actual attenuation of chemical transformations under these conditions. All reactions, with the exception of (R4), reverse their effect on the formation of the OH radical, and consequently τ, with a significant decrease in the corresponding values. At the same time, the moments of inversion of the influence of reactions (R1) and (R3) occur later than those of (R2) and (R5), but also earlier than the time $\tau(OH^*_{max})$ in all four cases. Overall, Fig. 7a shows that the magnitude of the τ value at relatively high temperatures is determined by reactions (R1), (R3), and (R4).

Simulation using the DKM from ref [29] (Fig. 7b) demonstrate that the influence of reactions R1 - R5 is the same as by the DKM from ref [32] (Fig. 7a). At the same time, the influence of the reaction, which is the only one in the DKM from ref [29] is noticeable

$$H_2 + O_2 = H + HO_2 \quad (R6)$$

Reaction R6 behaves symbate with reactions (R1), (R3), and (R4), the sensitivity to which is similar to the calculations [32] (Fig. 7a). In addition to the appearance of R6, a weak sensitivity to recombination reactions with OH formation is noticeable

$$O + H + M = OH + M \quad (R7)$$

and its decline

$$O + OH + M = H_2O + M \quad (R8)$$

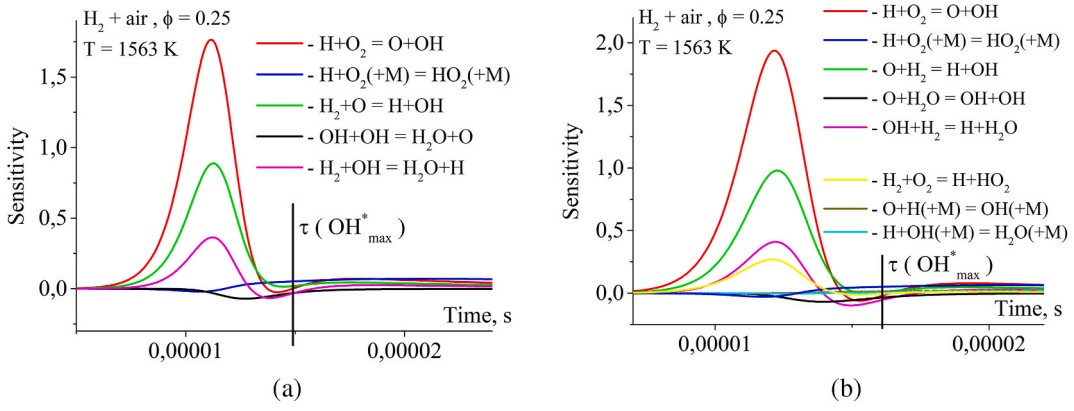

Fig. 7. Analysis of the local sensitivity of the main pathways of the formation and consumption of OH radicals during the combustion of a lean hydrogen-air mixture by the DKMs from refs [32] (a) and [29] (b). The experimental conditions are specified in the caption of Fig. 6b.

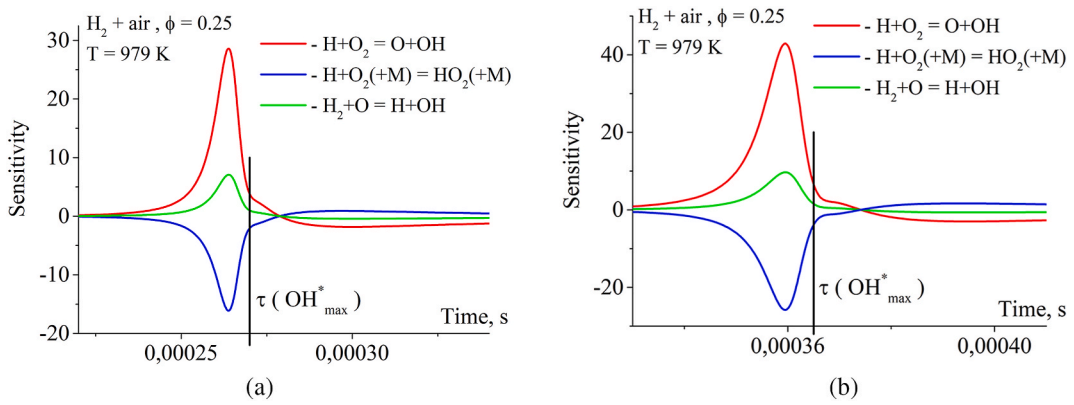

Fig. 8. Analysis of the local sensitivity of the main pathways of the formation and consumption of OH radicals during the combustion of a lean hydrogen-air mixture by the DKMs from refs [32] (a) and [29] (b). The experimental conditions are specified in the caption of Fig. 6a.

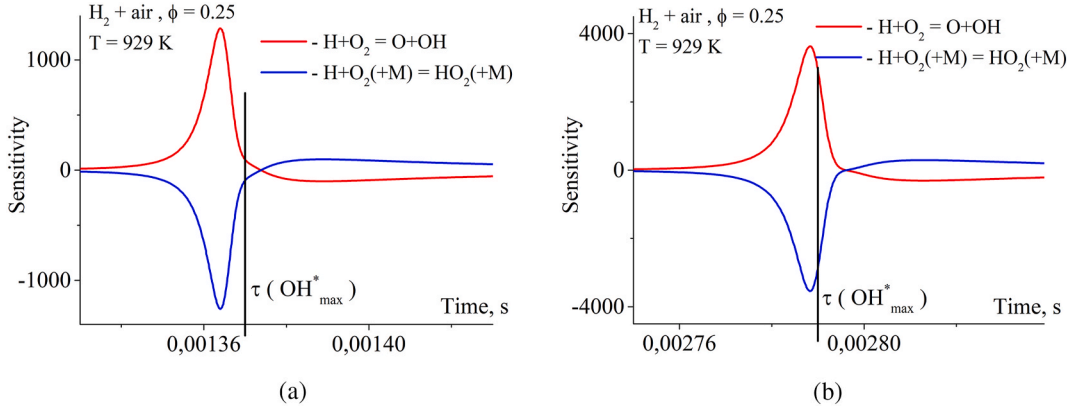

Fig. 9. Analysis of the local sensitivity of the main pathways of the formation and consumption of OH radicals during the combustion of a lean hydrogen-air mixture by the DKMs from refs [32] (a) and [29] (b). The conditions are: P = 1.03 atm, T = 929 K, φ = 025.

With decreasing temperature, the relative influence of reactions (R3) – (R5) on the formation of τ value decreases, and (R2) increases (Fig. 8). This leads to the fact that in the region of temperature 970 K, the influence of reactions (R4) and (R5) is not observed at all. The influence of reactions (R6) - (R8) in the calculations [29] also disappears. Fig. 8 shows that the times of reaching the maximum influence of reactions (R1) – (R3) actually coincide. The value $\tau(OH^*_{max})$, in contrast to Fig. 7, is reached before the reaction influence inversions occur. In contrast to the results of Fig. 7, the time moments of the influence inversions of the reactions (R1) – (R3) in Fig. 8 are close.

At transition to the region T < 970 K, the influence of reaction (R3) is completely absent and the whole process of τ value formation is determined mainly by the competition of reactions (R1) and (R2) (Fig. 9). In this region, one can see the complete symmetry of the influence of these two reactions, which is not the case at temperatures above 970 K (Figs. 7 and 8). At the same time, the calculations using DKMs from refs [32] and [29] show identical effects of (R1) and (R2). In this case, the value $\tau(OH^*_{max})$ it is reached, as in the case of Fig. 8, earlier than the inversions of the influence of reactions (R1) and (R2) occur.

Sensitivity analysis according to Figs. 6–8 showed that at T < 970 K, the autoignition activation energy is formed by the competition of reactions (R1) and (R2) only. As the temperature increases above 970 K, the influence of reaction R2 decreases, and the self-ignition activation energy is determined by reactions (R1), (R3), and (R4). These results support the statements presented in detail in [44].

The local sensitivity analysis shows that for the DKMs from refs [29, 32], no influence of reactions involving H_2O_2 is detected in the whole investigated temperature range. The negligible influence of H_2O_2 for a number of cases was also pointed out in [44]. This result leads to the desire to perform a reduction of DKMs from refs [29,32] by excluding H_2O_2 and the corresponding reactions involving it in the description of the induction period of ignition of lean and ultra-lean hydrogen-air mixtures. The procedure carried out in this way showed that for DKM from ref [32] it is quite justified for T > 920 K (see Table 2). The reactions R7, R8 and the recombination reaction of H atoms were also excluded. As a result, the DKM from ref [32] consisting of 21 reactions and 8 species (excluding OH* and reactions involving them) was reduced to a kinetic mechanism with 9 reactions with 7 components. In the case of DKM from ref [29], the exclusion of reactions involving H_2O_2 leads to bad result. Considering that DKM from ref [29] has only one

Table 2
Comparison of $\tau(OH^*_{max})$ calculated with the DKM from ref [32] and reduced kinetic mechanism (9 reactions with 7 species).

	φ = 0.15		φ = 0.25	
T, K	DKM	Reduced	DKM	Reduced
880	0.36	1.2	0.3	0.7
900	0.09	0.23	0.07	0.14
920	6.2e-3	7.3e-3	4.2e-3	4.9e-3
940	8.1e-4	7.9e-4	6.3e-4	6.2e-4
960	4.6e-4	4.5e-4	3.6e-4	3.5e-4
980	3.2e-4	3.1e-4	2.6e-4	2.5e-4
1000	2.5e-4	2.4e-4	2.0e-4	2.0e-4
1100	1.1e-4	1.1e-4	8.8e-5	8.9e-5
1200	6.4e-5	6.4e-5	5.2e-5	5.3e-5
1400	3.1e-5	3.1e-5	2.5e-5	2.6e-5
1700	1.5e-5	1.5e-5	1.2e-5	1.3e-5

initiation reaction R6 it can be said that the presence of a second initiation reaction with the formation of two OH radicals can replace reactions involving H_2O_2 in DKMs for lean hydrogen-air mixtures at initial atmospheric pressure.

5. Conclusion

In the presented study, it was possible to experimentally obtain reliable ignition delay (τ) values for lean (5.93% and 9.5% by volume) hydrogen-air mixtures in the temperature range of 902–1630 K at an initial pressure of 1 atm behind the reflected shock waves. Highly sensitive end-face technique for recording OH* emission in two shock tubes was used. Additionally, for the first-time data was obtained for a temperature range below 1000 K directly in the zone of changing influence of channels (R1) and (R2) on the formation of the ignition delay (τ) value. This made it possible to formulate approximation expressions for the calculation of ignition delay (τ) values in two temperature ranges below and above the temperature region as 970–980 K. For the studied mixtures in each interval, the corresponding values of activation energy were determined, which amount to 61.1 $\frac{KJ}{mole}$ in the region of high (more than 970–980 K) temperatures and $243 - 284$ $\frac{KJ}{mole}$ in the region of low (less than 970–980 K) temperatures. Numerical modelling of OH* signals was performed using three different independent DKMs described in the literature, and good agreement between the experimentally observed and calculated ignition delay (τ) values was demonstrated. The sensitivity analysis allowed us to show that self-ignition of lean and ultra-lean hydrogen-air mixtures can be described by a reduced kinetic mechanism in the absence of reactions involving H_2O_2, but in the presence of an initiation reaction with the formation of two OH radicals.

Declaration of competing interest

The authors declare that they have no known competing financial interests or personal relationships that could have appeared to influence the work reported in this paper.

Acknowledgements

The present study partially was carried out under a contract No. 87/21 (2021) with the Department of Nuclear and Radiation Safety of the Ministry of Emergency Situations of the Republic of Belarus (Gosatomnadzor).

Appendix A. Supplementary data

Supplementary data to this article can be found online at https://doi.org/10.1016/j.ijhydene.2024.03.363.

References

[1] Gharari R, Kazeminejad H, Mataji Kojouri N, Hedayat A. A review on hydrogen generation, explosion, and mitigation during severe accidents in light water nuclear reactors. Int J Hydrogen Energy 2018;43(4):1939–65. https://doi.org/10.1016/j.ijhydene.2017.11.174. ISSN 0360-3199.
[2] Tereza AM, Agafonov GL, Anderzhanov EK, et al. Numerical simulation of autoignition characteristics of lean hydrogen–air mixtures. Russ J Phys Chem B 2022;16:686–92. https://doi.org/10.1134/S1990793122040297.
[3] Yakovenko I, Kiverin A, Melnikova K. Ultra-lean gaseous flames in terrestrial gravity conditions. Fluid 2021;6:21. https://doi.org/10.3390/fluids6010021.
[4] Yakovenko IS, Ivanov MF, Kiverin AD, Melnikova KS. Large-scale flame structures in ultra-lean hydrogen-air mixtures. Int J Hydrogen Energy 2018;43(3):1894–901. https://doi.org/10.1016/j.ijhydene.2017.11.138. ISSN 0360-3199.
[5] Tereza AM, Agafonov GL, Anderzhanov EK, et al. Numerical simulation of autoignition characteristics of lean hydrogen–air mixtures. Russ J Phys Chem B 2022;16:686–92. https://doi.org/10.1134/S1990793122040297.
[6] Saji G. Root cause study on hydrogen generation and explosion through radiation-induced electrolysis in the Fukushima Daiichi accident. Nucl Eng Des 2016;307:64–76. https://doi.org/10.1016/j.nucengdes.2016.01.039. ISSN 0029-5493.
[7] Ng Hoi Dick, Lee John HS. Comments on explosion problems for hydrogen safety. J Loss Prev Process Ind 2008;21(2):136–46. https://doi.org/10.1016/j.jlp.2007.06.001. ISSN 0950-4230.
[8] Baranyshyn YA, Krivosheyev PN, Penyazkov OG, et al. Flame front dynamics studies at deflagration-to-detonation transition in a cylindrical tube at low-energy initiation mode. Shock Waves 2020;30:305–13. https://doi.org/10.1007/s00193-020-00937-0.
[9] Krivosheyev Pavel, Penyazkov Oleg, Sakalou Aliaksei. Analysis of the final stage of flame acceleration and the onset of detonation in a cylindrical tube using high-speed stereoscopic imaging. Combust Flame 2020;216:146–60. https://doi.org/10.1016/j.combustflame.2020.02.027. ISSN 0010-2180.
[10] Krivosheyev PN, Novitski AO, Penyazkov OG. Evolution of the reaction front shape and structure on flame acceleration and deflagration-to-detonation transition. Russ J Phys Chem B 2022;16:661–9. https://doi.org/10.1134/S1990793122040248.
[11] Krivosheyev Pavel, Novitski Alexey, Penyazkov Oleg. Flame front dynamics, shape and structure on acceleration and deflagration-to-detonation transition. Acta Astronaut 2023;204:692–704. https://doi.org/10.1016/j.actaastro.2022.10.016. ISSN 0094-5765.
[12] Krivosheyev PN, Penyazkov OG. On initial stage of combustion of acetylene–oxygen mixtures in a tube. Russ J Phys Chem B 2023;17:388–93. https://doi.org/10.1134/S1990793123020094.
[13] Yakovenko Ivan, Kiverin Alexey, Krivosheyev Pavel, Kuzmitski Viachaslau, Navitski Aliaksei, Penyazkov Oleg, Tyurnin Alexey, Yarkov Andrey. Burning rate estimation based on flame evolution in a channel. Acta Astronaut 2023;204:768–75. https://doi.org/10.1016/j.actaastro.2022.10.036. ISSN 0094-5765.
[14] Yarkov AV, Kiverin AD, Yakovenko IS. Flame acceleration in a channel: effects of the channel width and wall roughness. Combust Explos Shock Waves 2023;59:415–23. https://doi.org/10.1134/S0010508223040032.
[15] Kiverin AD, Tyurnin AV, Yakovenko IS. On the critical condition for flame acceleration in hydrogen-based mixtures. Materials 2023;16:2813. https://doi.org/10.3390/ma16072813.
[16] Kiverin AD, Turnin AV, Yakovenko IS. Scalability of flame propagation in a channel. Russ J Phys Chem B 2021;15:984–8. https://doi.org/10.1134/S1990793121060191.
[17] Kiverin AD, Smygalina AE, Yakovenko IS. The classification of the scenarios of fast combustion wave development and deflagration-to-detonation transition in channels. Russ J Phys Chem B 2020;14:607–13. https://doi.org/10.1134/S1990793120040168.
[18] Grune J, Sempert K, Haberstroh H, Kuznetsov M, Jordan T. Experimental investigation of hydrogen–air deflagrations and detonations in semi-confined flat layers. J Loss Prev Process Ind 2013;26(2):317–23. https://doi.org/10.1016/j.jlp.2011.09.008. ISSN 0950-4230.
[19] Smirnov NN, Nikitin VF, Mikhalchenko EV, Stamov LI, Tyurenkova VV, Smirnov NN. Evolution of the cellular structure of detonation waves under the condition of non-uniform initiation. Acta Astronaut 2023;213:156–67. https://doi.org/10.1016/j.actaastro.2023.08.036. ISSN 0094-5765.
[20] Smirnov NN, Azatyan VV, Nikitin VF, Mikhalchenko EV, Smirnova MN, Stamov LI, Tyurenkova VV. Control of detonation in hydrogen-air mixtures. Int J Hydrogen Energy 2023. https://doi.org/10.1016/j.ijhydene.2023.11.085. ISSN 0360-3199.
[21] Smirnov NN, Nikitin VF, Mikhalchenko EV, Stamov LI, Tyurenkova VV. Modelling cellular structure of detonation waves in hydrogen-air mixtures. Int J Hydrogen Energy 2023. https://doi.org/10.1016/j.ijhydene.2023.08.184. ISSN 0360-3199.
[22] Saxena Priyank, Williams Forman A. Testing a small detailed chemical-kinetic mechanism for the combustion of hydrogen and carbon monoxide. Combust Flame 2006;145(Issues 1–2):316–23. https://doi.org/10.1016/j.combustflame.2005.10.004. ISSN 0010-2180.
[23] Derevyago A, Penyazkov O, Ragotner K, Sevruk K. Auto-ignition of hydrogen-air mixture at elevated pressures. In: Hannemann K, Seiler F, editors. Shock waves. Berlin, Heidelberg: Springer; 2009. https://doi.org/10.1007/978-3-540-85168-4_118.
[24] Dryer Frederick L. Marcos Chaos, Ignition of syngas/air and hydrogen/air mixtures at low temperatures and high pressures: experimental data interpretation and kinetic modeling implications. Combust Flame 2008;152(Issues 1–2):293–9. https://doi.org/10.1016/j.combustflame.2007.08.005. ISSN 0010-2180.
[25] Chaos Marcos, Dryer Frederick. Syngas combustion kinetics and applications. Combust Sci Technol 2008;180:1053–96. https://doi.org/10.1080/00102200801963011.
[26] Pang GA, Davidson DF, Hanson RK. Experimental study and modeling of shock tube ignition delay times for hydrogen–oxygen–argon mixtures at low temperatures. Proc Combust Inst 2009;32(Issue 1):181–8. https://doi.org/10.1016/j.proci.2008.06.014. ISSN 1540-7489.
[27] Hong Zekai, Davidson David F, Hanson Ronald K. An improved H_2/O_2 mechanism based on recent shock tube/laser absorption measurements. Combust Flame 2011;158(4):633–44. https://doi.org/10.1016/j.combustflame.2010.10.002. ISSN 0010-2180.
[28] Schönborn Alessandro, Sayad Parisa, Konnov Alexander A, Klingmann Jens. OH*-chemiluminescence during autoignition of hydrogen with air in a pressurised turbulent flow reactor. Int J Hydrogen Energy 2014;39(23):12166–81. https://doi.org/10.1016/j.ijhydene.2014.05.157. ISSN 0360-3199.
[29] Kéromnès Alan, Metcalfe Wayne K, Heufer Karl A, Donohoe Nicola, Das Apurba K, Sung Chih-Jen, Herzler Jürgen, Naumann Clemens, Griebel Peter, Mathieu Olivier, Krejci Michael C, Petersen Eric L, Pitz William J, Curran Henry J. An experimental and detailed chemical kinetic modeling study of hydrogen and syngas mixture oxidation at elevated pressures. Combust Flame 2013;160(6):995–1011. https://doi.org/10.1016/j.combustflame.2013.01.001. ISSN 0010-2180.

[30] Pavlov VA, Gerasimov GY. Measurement of ignition limits and induction times of hydrogen–air mixtures behind the incident shock wave front at low temperatures. J Eng Phys Thermophys 2014;87:1291–7. https://doi.org/10.1007/s10891-014-1132-z.
[31] Alekseev Vladimir A, Christensen Moah, Konnov Alexander A. The effect of temperature on the adiabatic burning velocities of diluted hydrogen flames: a kinetic study using an updated mechanism. Combust Flame 2015;162(5):1884–98. https://doi.org/10.1016/j.combustflame.2014.12.009. ISSN 0010-2180.
[32] Vlasov PA, Smirnov VN, Tereza AM. Reactions of initiation of the autoignition of H_2–O_2 mixtures in shock waves. Russ J Phys Chem B 2016;10:456–68. https://doi.org/10.1134/S1990793116030283.
[33] Smith GP, Tao Y, Wang H. Foundational fuel chemistry model version 1.0 (FFCM-1). http://nanoenergy.stanford.edu/ffcm1; 2016.
[34] Hu Erjiang, Pan Lun, Gao Zhenhua, Lu Xin, Meng Xin, Huang Zuohua. Shock tube study on ignition delay of hydrogen and evaluation of various kinetic models. Int J Hydrogen Energy 2016;41(30):13261–80. https://doi.org/10.1016/j.ijhydene.2016.05.118. ISSN 0360-3199.
[35] Skrebkov SS Kostenko, Smirnov AL. Vibrational nonequilibrium and reaction heat effect in diluted hydrogen-oxygen mixtures behind reflected shock waves at 1000 < T < 1300 K. Int J Hydrogen Energy 2020;45(4):3251–62. https://doi.org/10.1016/j.ijhydene.2019.11.168. ISSN 0360-3199.
[36] Zhang Yongxiang, Fu Jianqin, Xie Mingke, Liu Jingping. Improvement of H_2/O_2 chemical kinetic mechanism for high pressure combustion. Int J Hydrogen Energy 2021;46(7):5799–811. https://doi.org/10.1016/j.ijhydene.2020.11.083. ISSN 0360-3199.
[37] Konnov Alexander A. Remaining uncertainties in the kinetic mechanism of hydrogen combustion. Combust Flame 2008;152(4):507–28. https://doi.org/10.1016/j.combustflame.2007.10.024. ISSN 0010-2180.
[38] Davidson D, Hanson R. Interpreting shock tube ignition data. Int J Chem Kinet 2004;36:510–23. https://doi.org/10.1002/kin.20024.
[39] Medvedev Sergey P, Agafonov Gennady L, Khomik Sergey V, Gelfand Boris E. Ignition delay in hydrogen–air and syngas–air mixtures: experimental data interpretation via flame propagation. Combust Flame 2010;157(7):1436–8. https://doi.org/10.1016/j.combustflame.2010.03.003. ISSN 0010-2180.
[40] Urzay Javier, Kseib Nicolas, Davidson David F, Iaccarino Gianluca, Hanson Ronald K. Uncertainty-quantification analysis of the effects of residual impurities on hydrogen–oxygen ignition in shock tubes. Combust Flame 2014;161(1):1–15. https://doi.org/10.1016/j.combustflame.2013.08.012. ISSN 0010-2180.
[41] Mulvihill Clayton R, Petersen Eric L. Concerning shock-tube ignition delay times: an experimental investigation of impurities in the H_2/O_2 system and beyond. Proc Combust Inst 2019;37(Issue 1):259–66. https://doi.org/10.1016/j.proci.2018.05.024. ISSN 1540-7489.
[42] Tereza AM, Agafonov GL, Anderzhanov EK, et al. Numerical simulation of the effect of additives on autoignition of lean hydrogen–air mixtures. Russ J Phys Chem B 2023;17:425–32. https://doi.org/10.1134/S1990793123020173.
[43] Medvedev S, Agafonov G, Khomik S. Low-temperature ignition delay for hydrogen–air mixtures in light of a reaction mechanism with quantum correction. Acta Astronaut 2016;126. https://doi.org/10.1016/j.actaastro.2016.04.019.
[44] Sánchez Antonio L, Williams Forman A. Recent advances in understanding of flammability characteristics of hydrogen. Prog Energy Combust Sci 2014;41:1–55. https://doi.org/10.1016/j.pecs.2013.10.002. ISSN 0360-1285.
[45] Fernández-Galisteo Daniel, Weiss Adam, Sánchez Antonio L, Williams Forman A. A one-step reduced mechanism for near-limit hydrogen combustion with general stoichiometry. Combust Flame 2019;208:1–4. https://doi.org/10.1016/j.combustflame.2019.06.018. ISSN 0010-2180.
[46] Hamid Hashemi, Christensen Jakob M, Sander Gersen, Glarborg Peter. Hydrogen oxidation at high pressure and intermediate temperatures: experiments and kinetic modeling. Proc Combust Inst 2015;35(Issue 1):553–60. https://doi.org/10.1016/j.proci.2014.05.101. ISSN 1540-7489.
[47] Olm Carsten, Zsély István Gy, Pálvölgyi Róbert, Varga Tamás, Nagy Tibor, Curran Henry J, Turányi Tamás. Comparison of the performance of several recent hydrogen combustion mechanisms. Combust Flame 2014;161(9):2219–34. https://doi.org/10.1016/j.combustflame.2014.03.006. ISSN 0010-2180.
[48] Konnov Alexander A. Yet another kinetic mechanism for hydrogen combustion. Combust Flame 2019;203:14–22. https://doi.org/10.1016/j.combustflame.2019.01.032. ISSN 0010-2180.
[49] Weydahl Torleif, Poyyapakkam Madhavan, Seljeskog Morten, Haugen Nils. Assessment of existing H_2/O_2 chemical reaction mechanisms at reheat gas turbine conditions. Fuel Energy Abstr 2011;36:12025–34. https://doi.org/10.1016/j.ijhydene.2011.06.063.
[50] Jin Shaoye, Shu Bo, He Xiaoyu, Fernandes Ravi, Li Liguang. A study on autoignition characteristics of H_2-O_2 mixtures with diluents of Ar/N_2 in rapid compression machine for argon power cycle engines. Fuel 2021;303:121291. https://doi.org/10.1016/j.fuel.2021.121291.
[51] Shimizu Kazuya, Hibi Atsushi, Koshi Mitsuo, Morii Youhi, Tsuboi Nobuyuki. Updated kinetic mechanism for high-pressure hydrogen combustion. J Propul Power 2011;27:383–95. https://doi.org/10.2514/1.48553.
[52] Mathieu A Levacque, Petersen EL. Effects of N_2O addition on the ignition of H_2–O_2 mixtures: experimental and detailed kinetic modeling study. Int J Hydrogen Energy 2012;37(20):15393–405. https://doi.org/10.1016/j.ijhydene.2012.07.071. ISSN 0360-3199.
[53] Zhang Yingjia, Huang Zuohua, Wei Liangjie, Zhang Jiaxiang, Law Chung K. Experimental and modeling study on ignition delays of lean mixtures of methane, hydrogen, oxygen, and argon at elevated pressures. Combust Flame 2012;159(3):918–31. https://doi.org/10.1016/j.combustflame.2011.09.010. ISSN 0010-2180.
[54] Pan Lun, Hu Erjiang, Deng Fuquan, Zhang Zihang, Huang Zuohua. Effect of pressure and equivalence ratio on the ignition characteristics of dimethyl ether-hydrogen mixtures. Int J Hydrogen Energy 2014;39(33):19212–23. https://doi.org/10.1016/j.ijhydene.2014.09.098. ISSN 0360-3199.
[55] Jiang Xue, Deng Fuquan, Pan Youshun, Sun Wuchuan, Huang Zuohua. Effect of hydrogen enrichment on the auto-ignition of lean n-pentane/Hydrogen mixtures at elevated pressure. Int J Hydrogen Energy 2020;45(55):31105–17. https://doi.org/10.1016/j.ijhydene.2020.08.004. ISSN 0360-3199.
[56] Linteris GT, Babushok VI. Promotion or inhibition of hydrogen–air ignition by iron-containing compounds. Proc Combust Inst 2009;32:2535–42. https://doi.org/10.1016/j.proci.2008.09.006.
[57] Donato Nicole S, Petersen Eric L. Simplified correlation models for CO/H_2 chemical reaction times. Int J Hydrogen Energy 2008;33(24):7565–79. https://doi.org/10.1016/j.ijhydene.2008.09.036. ISSN 0360-3199.
[58] Dinh Thi L, Nguyen Hoang V, Huang Z. To study on ignition characteristics of syngas mixtures by shock tube. SAE Technical Paper 2013-01-0118 2013. https://doi.org/10.4271/2013-01-0118.
[59] Wang Quande, Sun Yanjin, Curran HJ. Comparative chemical kinetic analysis and skeletal mechanism generation for syngas combustion with NO_x chemistry. Energy Fuels 2020;34(1):949–64. https://doi.org/10.1021/acs.energyfuels.9b03440.
[60] Michael JV, Sutherland JW, Harding LB, Wagner AF. Initiation in H2/O2: rate constants for H2+O2→H+HO2 at high temperature. Proc Combust Inst 2000;28 (Issue 2):1471–8. https://doi.org/10.1016/S0082-0784(00)80543-3. ISSN 1540-7489.
[61] CHEMKIN-Pro 15112. CK-TUT-10112-1112-UG-1. San Diego: Reaction Design; 2011.
[62] Burcat Alexander, Ruscic Branko. Third millennium ideal gas and condensed phase thermochemical database for combustion (with update from active thermochemical tables). No. ANL-05/20. Argonne, IL (United States): Argonne National Lab. (ANL); 2005.
[63] Moelwyn-Hughes EA. Chemical Kinetics and Chain Reactions. By N. Semenoff. Pp. xii, 480. 35s. 1935. International series of monographs on physicsOxford University Press). The Mathematical Gazette 1935;19(233):153–4. https://doi.org/10.2307/3608050.
[64] Baulch DL, Cobos CJ, Cox RA, Esser C, Frank P, Just Th, Kerr JA, Pilling MJ, Troe J, Walker RW, Warnatz J. Evaluated kinetic data for combustion modelling. J Phys Chem Ref Data 1992;21(3):411. https://doi.org/10.1063/1.555908.